Journal of Cellular Biochemistry 90:819–836 (2003)

Rho Exchange Factor ECT2 Is Induced by Growth Factors and Regulates Cytokinesis Through the N-Terminal Cell Cycle Regulator-Related Domains

Shin'ichi Saito,[1] Takashi Tatsumoto,[1,2] Matthew V. Lorenzi,[1] Marcio Chedid,[1] Veena Kapoor,[1] Hiromi Sakata,[1] Jeffrey Rubin,[1] and Toru Miki[1,2]*

[1]Laboratory of Cellular and Molecular Biology, National Cancer Institute, Bldg. 37-1E24, 37 Convent Dr., Bethesda, Maryland 20892-4255
[2]Molecular Tumor Biology Section, Basic Research Laboratory, National Cancer Institute, Bldg. 37-1E24, 37 Convent Dr., Bethesda, Maryland 20892-4255

Abstract The *ECT2* protooncogene plays a critical role in cytokinesis, and its C-terminal half encodes a Dbl homology-pleckstrin homology module, which catalyzes guanine nucleotide exchange on the Rho family of small GTPases. The N-terminal half of ECT2 (ECT2-N) contains domains related to the cell cycle regulator/checkpoint control proteins including human XRCC1, budding yeast CLB6, and fission yeast Cut5. The Cut5-related domain consists of two BRCT repeats, which are widespread to repair/checkpoint control proteins. ECT2 is ubiquitously expressed in various tissues and cell lines, but elevated levels of ECT2 expression were found in various tumor cell lines and rapidly developing tissues in mouse embryos. Consistent with these findings, induction of ECT2 expression was observed upon stimulation by serum or various growth factors. In contrast to other oncogenes whose expression is induced early in G1, ECT2 expression was induced later, coinciding with the initiation of DNA synthesis. To test the role of the cell cycle regulator/checkpoint control protein-related domains of ECT2 in cytokinesis, we expressed various ECT2 derivatives in U2OS cells, and analyzed their DNA content by flow cytometry. Expression of the N-terminal half of ECT2, which lacks the catalytic domain, generated cells with more than 4N DNA content, suggesting that cytokinesis was inhibited in these cells. Interestingly, ECT2-N lacking the nuclear localization signals inhibited cytokinesis more strongly than the derivatives containing these signals. Mutational analyses revealed that the XRCC1, CLB6, and BRCT domains in ECT2-N are all essential for the cytokinesis inhibition by ECT2-N. These results suggest that the XRCC1, CLB6, and BRCT domains of ECT2 play a critical role in regulating cytokinesis. J. Cell. Biochem. 90: 819–836, 2003.

Key words: cell division; mitogen; serum induction; small GTPase; oncogene

The epithelial cell transforming gene 2 (*ECT2*) protooncogene was isolated from a mouse epithelial cell line BALB/MK as a cDNA clone, which confers transforming activity in fibroblasts through an expression cloning strategy [Miki et al., 1993]. The transforming activity of ECT2 is activated by the truncation of its N-terminal half. The C-terminal half

Abbreviations used: BRCT, BRCA1 C-terminal; CLB6, cyclin B6; Cut5, cells untimely torn 5; DH, Dbl homology; *ECT2*, epithelial cell transforming gene 2 (human); *ect*2, mouse *ECT2*; ECT2-N, N-terminal half of ECT2 protein; EGF, epidermal growth factor; GFP, green fluorescent protein; HGF, hepatocyte growth factor; IGF-I, insulin-like growth factor I; KGF, keratinocyte growth factor; PH, pleckstrin homology; SF, scatter factor; TGF-β, transforming growth factor-β

Grant sponsor: Japan Society of Promotion of Sciences fellowships (in NIH).

Shin'ichi Saito's present address is Laboratory of Cell Biology, National Cancer Institute, Bethesda, MD.

Takashi Tatsumoto's present address is Fukuoka Teishin Hospital, 2-6-11 Yakuin, Chuo-ku, Fukuoka 810-8798, Japan.

Matthew V. Lorenzi's present address is Oncology Drug Discovery, Pharmaceutical Research Institute Bristol-Myers Squibb, P.O. Box 4000, Princeton, NJ 08543-4000.

Hiromi Sakata's present address is Institute of Artificial Organ, Transplantation and Gene Therapy, Sapporo Hokuyu Hospital, 6-6 Higashi Sapporo, Shiroishi-ku, Sapporo 090-8666, Japan.

*Correspondence to: Toru Miki, Building 37 Room 1D22, National Institutes of Health, 37 Convent Dr. MSC 4255, Bethesda, MD 20892-4255. E-mail: toru@helix.nih.gov

Received 27 June 2003; Accepted 15 August 2003

DOI 10.1002/jcb.10688

of ECT2 contains Dbl homology (DH) and pleckstrin homology (PH) domains, which are found in guanine nucleotide exchange factors of the Rho family of small GTP-binding proteins. The Rho family of small GTPases, represented by RhoA, Rac1, and Cdc42, function as molecular switches of diverse biological functions, such as cytoplasmic actin reorganization, cell motility, cell scattering, cytokinesis, lymphocyte coaggulation, smooth muscle contraction, and superoxide generation [Van Aelst and D'Souza-Schorey, 1997; Hall, 1998]. The GTP-bound form of Rho proteins is active, whereas the GDP-bound form is inactive. Activation of the Rho proteins is promoted by guanine nucleotide exchange factors (GEFs), which catalyze the replacement of bound GDP by GTP. The GTP-bound form of Rho proteins can specifically interact with their effectors or targets and transmit signals to downstream molecules. Rho proteins are inactivated through the hydrolysis of bound GTP to GDP by the intrinsic GTPase activity, assisted through GTPase activating proteins (GAPs).

We have shown that ECT2 catalyzes guanine nucleotide exchange on RhoA, Rac1, and Cdc42 in vitro [Tatsumoto et al., 1999]. ECT2 is a nuclear protein in interphase cells and then disperses in the cytoplasm after nuclear membrane breakdown. ECT2 is phosphorylated in G2 and M phases of the cell cycle. In M phase, ECT2 is localized in the mitotic spindle. During cytokinesis, ECT2 is localized in the midbody. Inhibition of the ECT2 function, either by microinjection of affinity-purified anti-ECT2 antibody or expression of a dominant-negative form of ECT2 (ECT2-N), strongly inhibits cytokinesis. A *Drosophila* gene *pbl*, whose mutation renders cells defective in cytokinesis during embryogenesis, encodes an ECT2-related protein [Prokopenko et al., 1999]. Therefore, ECT2 regulates cytokinesis from fly to humans. The level of GTP-bound, active form of Rho, does not change from S phase to prometaphase, but increases thereafter and reaches to a peak at telophase. ECT2 appears to play a critical role in the Rho activation during cytokinesis, as a dominant negative ECT2 efficiently inhibits the elevation of active Rho during cytokinesis [Kimura et al., 2000]. *ECT2* expression is induced in regenerating mouse liver after hepatectomy [Sakata et al., 2000]. Through somatic cell analysis and FISH, we have mapped the human *ECT2* gene to 3q26.1-q26.2 [Takai et al., 1995].

In this report, we show high levels of ECT2 expression in various tumor cell lines and rapidly proliferating cells in embryonic tissues. Consistent with this finding, ECT2 expression was regulated by serum and various mitogens. We also report that cytoplasmic localization of ECT2-N strongly enhances its activity to inhibit cytokinesis. Finally, we found that the cell cycle regulator-related domains are essential for the inhibition of cytokinesis by ECT2-N.

MATERIALS AND METHODS

DNA Constructs

Human ECT2 cDNA was isolated from a B5/589 human mammary epithelial cell cDNA library using the mouse *ect*2 cDNA as probe. The entire nucleotide sequence of the longest cDNA insert (clone 1M) was determined. This cDNA (4,349 nucleotides) contained a large open-reading frame encompassing 2,649 nucleotides (882 amino acids) beginning with a methionine coden at position 44S and ending with a TGA termination coden at position 3091, and was flanked by 5′- and 3′-untranslated regions. The segment was degssiter GenBank (Accession no. AY376439).

ECT2 N-terminal fragments were amplified by PCR using ECT2 clone 1M as template and subcloned between *BamH*I and *EcoR*I sites of the mammalian expression vector pcDNA3 (Invitrogen, CA) or pCEV29F3 [Lorenzi et al., 1999]. A small deletion was introduced in the Clb6-homology domain of ECT2-N4 by digestion with *BspE*I and *EcoN*I followed by blunt-end ligation. The THL to AAA mutations in the BRCT-1 and BRCT-2 domains were introduced by PCR using mutant primers. pEGFP-C1 was from Clontech, CA. All constructs generated by PCR were sequenced to ensure no mutation occurred except the designed mutations.

Cell Culture

U2OS cells were grown in modified McCoy's 5A medium supplemented with 15% fetal bovine serum. Other cell lines were maintained in Dulbecco's modified minimal essential medium (Invitrogen, CA), supplemented with 10% fetal bovine serum, 100 nM glutamine, and penicillin/streptomycin in a humidified atmosphere with 5% CO_2. For growth factor treatment, NIH/3T3 mouse embryonic fibroblasts and Balb/MK

mouse epidermal keratinocytes were switched to serum-free medium [1:1 (v/v) mixture of Dulbecco's modified Eagle's medium (DMEM) and Ham's F-12 medium, supplemented with 5 μg/ml transferrin and 30 nM Na_2SeO_3] and incubated overnight. The growth factors used in this study were all human recombinant proteins. KGF and HGF/SF were purified as previously described [Ron et al., 1993; Cioce et al., 1996]. TGF-β was purchased from R&D (Minneapolis, MN). EGF and IGF-I were from Pepro Tech, Inc. (Rocky Hill, NJ). DNA synthesis was assessed by measuring ^{3}H-thymidine incorporation as described [Rubin et al., 1989].

Cell Cycle Analysis by Multi-Parameter Flow Cytometry

Cells (10^6/dish) were seeded in 10-cm dishes and cotransfected following day with 10 μg of the indicated expression vector DNA and 1 μg of the selection marker plasmid pcDNA3-CD56 [Saito et al., 1994]. At the indicated time points, cells were washed once with phosphate buffered saline (PBS) and once with PBS containing 0.1% EDTA, and then incubated in PBS containing 0.1% EDTA for 5 min at 37°C to detach from plates. The detached cells were collected by centrifugation, resuspended in 100 μl of medium containing 4 μg of ITK-2 (anti-CD56 antibody) [Saito et al., 1991], and then incubated on ice for 30 min. After washing twice with medium, cells were incubated with FITC-conjugated anti-mouse IgG (Roche, IN) on ice for 20 min, followed by washing twice with PBS. For cell cycle analysis, cells were fixed and stained with propidium iodide. At least 5,000 of CD56 positive cells were analyzed by a flow cytometer.

Immunoblot Analysis

Western blot analysis was performed with a polyclonal rabbit ECT2 antibody as previously reported [Tatsumoto et al., 1999]. Briefly, membranes were first blocked with 5% nonfat dry milk in PBS-Tween buffer (1.5 mM $NaH_2PO_4{\cdot}H_2O$, 8 mM Na_2HPO_4, 0.15 M NaCl, pH 7.4, 0.1% Tween-20), and rinsed in PBS-T. Next, the membranes were stained for 90 min at room temperature with a 1:2,000 dilution of affinity purified anti-ECT2 antibody. In addition to ECT2, separate membranes were probed with a 1:2,000 dilution of α-tubulin antibody. Bound antibody was detected by chemiluminescence using an ECL detection kit (Amersham).

In Situ Hybridization

In situ hybridization, studies for the detection of *ect2* transcript were performed as described [Fox and Cottler-Fox, 1993]. Briefly, 6-μm sections of formaldehyde fixed liver from Balb/c mice and 14-day-old embryos from C57BL/6 mice were prepared and mounted on silanized slides. The slides were cleared and prehybridized with ^{35}S-labeled sense or antisense probes prepared from *ect2* CL7 cDNA [Miki et al., 1993] as template. Some of the sections were also digested with proteases prior to hybridization. The slides were washed, dried, and coated with NBT2 Kodak emulsion. After 4-day exposure, the slides were developed and stained with hematoxylin and eosin. In all cases, background levels were within the acceptable range. Slides were examined with low power dark field and bright field microscopy.

Serum Induction of ECT2 in T98G Cells

T98G (ATCC CRL-1690), a human glioblastoma cell line, was obtained from the American Type Culture Collection (Manasas, VA) and cultured in Dulbecco's modified minimal essential medium (DMEM) (Invitrogen Corp., Carlsbad, CA) supplemented with 10% fetal bovine serum, 100 nM glutamine and penicillin/streptomycin. For synchronization, T98G cells at 70% confluence were placed in medium containing 0.1% fetal bovine serum (FBS) for 72 h, then split at the 1:3 ratio and released from starvation arrest by the addition of FBS to a final concentration of 10%. Progression through the cell cycle was monitored by measuring DNA content with flow cytometer as described. Samples were harvested at the indicated times and analyzed by Northern blotting with ECT2-N4 cDNA probe or Western blotting using anti-ECT2 antisera, anti-cyclin B1 (Santa Cruz, GNS1), anti-CDC2 (Santa Cruz, 17), and anti-α-tubulin (Oncogene Research Products, Ab-1).

RESULTS

N-Terminal Domain of ECT2 Is Related to Cell Cycle Regulators

We isolated human ECT2 using murine ect2 cDNA as template (Fig. 1). The structure of human ECT2 cDNA has been briefly reported [Tatsumoto et al., 1999]. Comparison of human

A

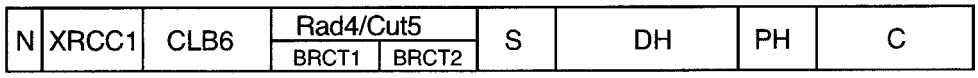

B

```
     1                                                  50
Hs   MAENSVLTST TGRTSLADSS IFDSKVTEIS KENILIGSTS YVEEMPQIET
Mm   ~~~~~~~~~~ ~~~~~~~~~~ ~~~~~~~~~~ ~~~~~~~~~~ ~~~~~~~~~~
Dm   ~~~~~~~~~~ ~~~~~~~~~~ ~~~~~~~~~M EMETIEEQSK CEMSITTLPT
Ce   ~~~~~~~~~~ ~~~~~~~~~~ ~~~~~~~~~M DVSMLQSPQK RIKTIQKLAV
     51                                                 99
Hs   RVILVQEAGK QEELIKALKD .IKVGFVKME SVEEFEGLDS PEFENVFVVT
Mm   ~~~~~~~~~~ ~~~~~~~~~~ ~~~~~~~~~~ ~~~~~~~~~~ ~~~~~~~~~~
Dm   RICLVGGVGQ DADTLQAAES .FGLPIVTSD TGLDILG.ES SDWRTFYVLD
Ce   SKKDVHDFKD IFEMLEEQKE KKNINIIQYD SLDDLSGDWS ...EYTFFCG
     100                                                143
Hs   DFQDSVFNDL YKADCR.... VIGPPVVLNC SQKGEPLP.. FSCRPLYCTS
Mm   ~~~~~~~~~~ ~~~~~~~~~~ ~~~~~~~~~~ ~~~~~~~~~~ ~~~~~~~~~~
Dm   DFEGASFEAI HKQKEC.... ILGPPALKYA AEMKQTLG.. QNSRPIYNYA
Ce   NFDSDLFRTL TKHQETQALF IIGASVLKNK LLKNEDLMTL RAARPLYCEL
     144                                          ***   192
Hs   MMNLVLCFTG .FRKKEELVR LVTLVHHMGG VIRKDFNSKV THLVANCTQG
Mm   MLNLVLCFTG .FRKKEELVK LVTLVHHMGG VIRKECNSKV THLVANCTQG
Dm   MRGVVTCFTG .IRKKDELTK LVNLIHSMGG CIKKDLNTKT THLICNHSGG
Ce   MKDVTMKLAA EVPNKRE... LVDLVHYMGG SVRKDTVSRT NVFIAAKVEA
     193                                                242
Hs   EKFRVAVSLG TPIMKPEWIY KAWERRNEQD FYAAVDDFRN EFKVPPFQDC
Mm   EKFRVAVSLG TPIMKPEWIY KAWERRNEQC FCAAVDDFRN EFKVPPFQDC
Dm   EKYQYAKTFR LTVVRPAWVF AAWADRNSLE FDATQENFTK THRLKAPEGQ
Ce   .KVQSISLVG VPTMRADWVT ECWKHRDDSY FDVMEPCFVD KHRLGVPEGL
     243                                   ***          291
Hs   ILSFLGFSDE EKTNMEEMTE MQGGKYLPLG DERCTHLVVE .ENIVKDLPF
Mm   ILSFLGFSDE EKHSMEEMTE MQGGSYLPVG DERCTHLIVE .ENTVKDLPF
Dm   KICFFGFPVE EHQHMVDVLL ENGGVCAELD DPECSHVVVD .EHTTLTKPE
Ce   SLFFHGFKQT EIDDMLRSLE NTGGKLAP.S PTLATHVVYN PDNDEVETLA
     292                                                336
Hs   EPSKKLYVVK QEWFWGSIQM DARAGETMYL Y.....EKAN TPELKKSVSM
Mm   EPSKKLFVVK QEWFWGSIQM DARAGETMYL Y.....EKAN TPELKKSVSL
Dm   PKNNHTHILK SDWFWYTIQ. NGYANEMDYL FGDYLDSITN TPNTDRRDSL
Ce   VSSNQVHVTK .EWFWVSLHR GCCAIEDNFA LP........ TGKLHRKPLE
     337                                                384
Hs   .LSLNTPNSN RKRRRLKETL AQLSRETDVS PFPPRKRPSA EHSLSI.GSL
Mm   .LSLSTPNSN RKRRRLKETL AQLSRETDLS PFPPRKRPSA EHSLSI.GSL
Dm   PISFN....K RKRKRFSQRI .QL.EGTPLG SGKRRSSVSD AGLLSVSNSL
Ce   SSSVSSPIGK SLRSQNSRSL SSMRD..... .......... ...CSVEGPT
     385                                                434
Hs   LDISNTPESS INYGDTPKSC TKSSKSSTPV PSKQSARWQV AKELYQTESN
Mm   LDISNTPESS IHYGETPKSC AKSSRSSTPV PPKQSARWQV AKELYQTESN
Dm   FDCTTSPDKL ....ESDKLL HAEPEASDAT PAKKSMRFNH FMDFYTTESN
Ce   .SLNMTPDYI YSNDDVENSC KS........ PRQPSKRLRV CMEMVETEKN
     435                                                483
Hs   YVNILATIIQ LFQVPLEEEG QRGGPILAPE EIKTIFGSIP DIFDVHTKI.
Mm   YVNILATIIQ LFQVPLEEEG QRGGPILAPE EIKTIFGSIP DIFDVHMKI.
Dm   YVGILDTILN LFKNKLEELA ETNDPLLNKS EIKTIFGNFL PIHEVHQSM.
Ce   YLSLLKLVVK .FKEALECEI SHNE.FMSRS DVAMMFGKLD PILELHERIF
     484                                                521
Hs   ......KDDL EDLIV..... .NWDESKSIG DIFLKYSKDL VKTYPPFVNF
Mm   ......KDDL EDLIA..... .NWDESRSIG DIFLKYAKDL VKTYPPFVNF
Dm   ......LEHL RKLHA..... .NWRERDCLIG DIIIQHRDEL IKAYPPYVNF
Ce   ARLTVMSNEA NTLLTVVNGK KNDDKNLDFA QVWIDAKEEM KKAYPQYINS

     522                                                571
Hs   FEMSKETIIK CEKQKPRFHA FLKINQAKPE CGRQSLVELL IRPVQRLPSV
Mm   FEMSKEMIIK CEKQKPRFHA FLKINQAKPE CGRQSLVELL IRPVQRLPSV
Dm   FEQMKEQLQY CDREYPRFHA FLKINQTKPE CGRQGLQDLM IRPVQRLPSI
Ce   YDTIKRLFDK QDRENSKFHT FCKAKESNPE FHRLKLTDLM VKPVQRLPSV
     572                                                621
Hs   ALLLNDLKKH TADENPDKST LEKAIGSLKE VMTHINEDKR KTEAQKQIFD
Mm   ALLLNDLKKH TADENPDKST LEKAIGSLKE VMTHINEDKR KTEAQKQIFD
Dm   SLLLNDILKH TTSGNADHGR LEEALKAIKQ VTLHINEDKR RTESRMAIFD
Ce   ILLLKEMAK. .KSDSKLKNN AEEAAKAIDE VLKTANKTRE KNDNFISHLS
     622                                                669
Hs   VVYEVDGCPA NLLSSHRSLV QRVETISLGE HPCDRGE..Q VTLFLFNDCL
Mm   VVYEVDGCPA NLLSSHRSLV QRVETVSLGE HPCDRGE..Q VTLFLFNDCL
Dm   IFNDIEGCPA HLVSSNRSFI LKCEVNELSD SLSGRGD..S LVLYLFSDSI
Ce   KFTDIENVPP ILVAANRMFI RELVVSPIAS TSPGLQQFAK MKLFLFHDVL
     670                                                711
Hs   EIARKRHKV. .......IGT FRSPHGQTRP PASLKHIHLM PLSQIKKVLD
Mm   EIARKRHKV. .......IGT FRSPHDRTRP PASLKHIHLM PLSQIKKVLD
Dm   ELCKRRSKG. .......FNT AKSP....ST AKTHKHLKLI SLNTIRLVID
Ce   IITKIRSEKN TMQRLARHAS FASLHSRQRR P..YRYIDQI QLNTMRSAFR
     712                                                751
Hs   IRETEDCHNA FALLVRPPTE QANVLLSFQM TSD..... ...ELPKENW
Mm   IRETEDCHNA FALLVRPPTE QANVLLSFQM TSE..... ...ELPKESW
Dm   I...SDSPRA FGLLLRGDKE K...LYTFTI SDE..... ...ETDKSVY
Ce   IRAPDEIAKC LELQQQNGST KPNVFVWCLI HRDEQGGDID TVFESNDDEE
     752                                                799
Hs   LKMLCRHVAN TICKADAENL IYTADPESF. EVNTKDMD.S TLSRASRAIK
Mm   LKMLCRHVAN TICKADAENL MYVADPESF. EVNTKDMD.S TLSRASRAIK
Dm   VKKLCNQIAA HTCRTDADKL LICRTSQEL. EVDISDVNVS TLSKAFKLAA
Ce   VRDFLDDIHV KIL.SDCGRF FYSSDPSDMN EINDAMVSDM T.TRYFRNLC
     800                                                846
Hs   KTSKKVTRAF SFSKTP...K RALRRALMTS HGSVEGRSPS SNDKHVMSRL
Mm   KTSKKVTRAF SFSKTP...K RALRMALSSS HSS.EGRSPP SSGKLAVSRL
Dm   KTRLKVGRAF SFNKTPNKLK RAVSTMMTSP FGSTNSLTPA S..QLAQMRL
Ce   GAKPQYGHGS QMNITVSE.. ....RSTQNE WSHNESFMPP PQSQSRMRRA
     847                                          882
Hs   SSTSSLAGIP SPSLVSLPSF FERRSHT... .LSRSTTHLI ~~~~~~~~~~
Mm   SSTSSLAGIP SPSLVSLPSF FERRSHT... .LSRSTTHLI ~~~~~~~~~~
Dm   ASCTNINEVD DEDCASM... ...RSSS... .PSTQSEMLV VPPLSVQPTR
Ce   FSNAQL.... ..TLATTLGF GRNQSRNNLG QINENTTFLQ SPRVSCDPAA

Hs   ~~~~~~~~~~ ~~~~~~~~~~ ~~~~~~~~~~ ~~~~~~~~~~ ~~~~~~~~~~
Mm   ~~~~~~~~~~ ~~~~~~~~~~ ~~~~~~~~~~ ~~~~~~~~~~ ~~~~~~~~~~
Dm   KNKAVVGRI~ ~~~~~~~~~~ ~~~~~~~~~~ ~~~~~~~~~~ ~~~~~~~~~~
Ce   LANMTSVGGL PGCQSESEST PKRGIRSRLT STTFLGGRHN ILGRNTSMRR
     1001                 1025
Hs   ~~~~~~~~~~ ~~~~~~~~~~ ~~~~~
Mm   ~~~~~~~~~~ ~~~~~~~~~~ ~~~~~
Dm   ~~~~~~~~~~ ~~~~~~~~~~ ~~~~~
Ce   QATGFAHSEK ELPRSKTSSY RVTDI
```

Fig. 1. Structure of human ECT2 protein deduced from the cDNA sequence. **A**: Schematic representation of ECT2 protein. BRCT, BRCA1 C-terminal repeat; CLB6, Cyclin B6 homology; DH, Dbl homology; PH, pleckstrin homology, S, small central domain. **B**: Comparison of amino acid sequences of ECT2 homologs of different species. The predicted amino acid sequence of human ECT2 (Hs) was compared with mouse Ect2 (Mm; [Miki et al., 1993]), *Drosophila* Pbl (Dm; [Prokopenko et al., 1999]), and *C. elegans* T19E10.1b (Ce; accession no. Z46795). Amino acid residues identical to those of human ECT2 are shown in bold. Amino acids are numbered from the first methionine coden of human ECT2. ''~,'' not present in the sequence; ''.,'' a gap introduced to maximize the alignment. The positions of the BRCT1 and BRCT2 mutations are shown by ''***'' (see Fig. 9A). **C**: Structural similarity of the N-terminal domain of ECT2 with related proteins. The human Rad4-like gene (accession no. D87448), *C. elegans* genes F37D6.1 (Z75540) and T19E10.1 (Z46795), and fission yeast Rad4/Cut5 (D16627), were first identified as proteins related to the N-terminal domain of ECT2 using BLAST, and then aligned by PILEUP in the Wisconsin package. Amino acid residues identical to those of human ECT2 are shadowed. Gaps are introduced to maximize the alignment.

ECT2 with related molecules revealed that murine *ect2* is the most closely related molecule (95% similarity, 84% identity at the amino acid level), although the human clone contained an additional stretch of 150 amino acids at its N-terminus. T19E10.1b, an open-reading frame identified by a *Caenorhabditis elegans* genome project, and *pebble* [Prokopenko et al., 1999],

Fig. 1. (*Continued*)

a recently identified *Drosophila* gene which regulates cytokinesis, exhibited similarities along with the entire coding sequence, suggesting that these genes are *C. elegans* and *Drosophila melanogaster* orthologs of human *ECT2*, respectively.

The N-terminal half of ECT2 was homologous to several cell cycle control proteins. Amino acids 76–139 exhibited homology to a yeast B-type cyclin, Clb6 [Schwob and Nasmyth, 1993] (29% identity, 54% similarity). This Clb6 homology region is followed by another domain that consists of two direct repeats and exhibits similarity to a fission yeast cell cycle regulator, Rad4/Cut5 [Saka and Yanagida, 1993]. Rad4/Cut5 is required for S phase entry as well as inhibition of M phase entry before completion of DNA synthesis, and plays a critical role in replication checkpoint control [Saka et al., 1994]. The Cut5-homology domain of ECT2 consisted of two BRCA1 C-terminal (BRCT) repeats, which are widespread in DNA damage-responsive cell cycle checkpoint or DNA repair proteins [Bork et al., 1997]. The ECT2 BRCT repeats were also related to those of the human topoisomerase II-binding protein TopBP1 [Yamane et al., 1997] and a human repair protein XRCC1 [Thompson et al., 1990]. Besides the BRCT homology, the very N-terminal region of ECT2 (amino acids 24–60) also exhibited another homology to XRCC1, and this region is designated XRCC1 homology domain (Fig. 1A). In addition to these genes, three genes identified by genome projects were found to exhibit sequence similarity to the ECT2 N-terminal domain (Fig. 1C). Among them, the human Rad4-like gene (accession no. Z46795) was most homologous to ECT2 in this region (28% identity, 46% similarity) in an overlap to

300 amino acids. A *C. elegans* gene identified by a genome project, F37D6.1 (accession no. Z75540), also contained structural similarity with the N-terminal region of ECT2. These results indicated that the combination of XRCC1, Clb6- and Rad4/Cut5-homology domains are well conserved in species and may exhibit cell cycle control functions in these organisms.

ECT2 Is Expressed at High Levels in Various Tumor Cells

To investigate the possible involvement of *ECT2* in human tumorigenesis, *ECT2* expression in human tumor cell lines was examined by Northern blot hybridization (Fig. 2A). RNAs from normal cells, a human embryonic fibroblast cell line M426 and a breast epithelial cell line B5/589, were included in each blot as controls. The human ECT2 cDNA probe detected a single message of 4.4 kb in normal as well as tumor cell lines. Interestingly, the majority of tumor cell lines showed higher ECT2 mRNA expression than the normal cells. In particular, liver, lung, bladder, and ovarian tumor cells showed high levels of ECT2 expression. A lung cancer cell line, A549, showed the highest ECT2 expression among all the cell lines tested. Whereas, higher expression was found in many tumor cells when compared to normal cells, no significant change in the size of ECT2 transcripts was observed. The cells showing higher ECT2 mRNA expression levels were subjected to Western analysis to test the protein expression levels. As shown in Figure 2B, several tumor cell lines expressed ECT2 protein at higher levels than normal fibroblasts (M426) or epithelial cells (B5/589). The lung carcinoma cell line, A549, which showed the highest ECT2 mRNA expression, also showed the highest protein expression. Several cell lines including HA188 (lung carcinoma), KATO III (gastric carcinoma), SKLMS (leiomyosarcoma), A431 (epidermoid carcinoma), and C33A (cervical carcinoma) also showed high levels of ECT2 protein expression. To test whether overexpression of ECT2 in these cells is attributed to gene amplification, genomic DNA was extracted from A549, HA146, HA188, HA1182, SW1271, and KATO III cells as well as B5/589 for a control. The DNAs were digested with *EcoR*I or *Hind*III and subjected to Southern analysis using ECT2 cDNA as probe. However, no alteration of intensity or size of the bands was detected (data not shown), indicating that the *ECT2* overexpression is not due to the amplification of *ECT2* locus in these cells.

ECT2 Is Expressed at High Levels in Rapidly Proliferating Cells During Fetal Development

We previously reported that *ect2* is expressed in limited numbers of adult mouse organs including kidney, liver, spleen, and testis and is not detected in brain, heart, lung, and skeletal muscle [Miki et al., 1993]. In order to determine the tissue distributions of the *ect2* transcripts during embryonic mouse development, serial sections of 14-day mouse embryo were examined by in situ hybridization. As shown in Figure 3A, strong signal of *ect2* mRNA was detected in brain, specifically in ventricular zone, olfactory lobe, and diencephalon. *Ect2* was also expressed in hematopoietic organs such as fetal liver and thymus, and proliferating epithelial cells including nasal cavity and gut. Moreover, we found *ect2* expression in primordia of tooth, costal cartilage, heart, lung, and pancreas. No specific hybridization was seen using sense strand probes (Fig. 3B). These results indicate that *ect2* mRNA expression occurs at sites of active cell proliferation in the developing organism.

ECT2 Expression Is Induced From S to M Phases by Serum

High level expression of *ECT2* in tumor cell lines and rapidly proliferating cells in embryonic tissues suggested that ECT2 expression is accompanied by rapid proliferation. Together with the presence of cell cycle regulator homology domains, *ECT2* expression may be regulated in a cell cycle specific manner. To test this possibility, confluent monolayers of M426 lung embryonic fibroblasts were cultured for 24 h in serum-free medium and then switched to culture medium containing 10% fetal bovine serum. As shown in Figure 4A, whereas anti-ECT2 stained serum-starved cells very faintly, the strong signal was detected in the nuclei of serum-induced cells. This staining was efficiently blocked when the antibodies were preincubated with recombinant ECT2 (data not shown), indicating that the staining was specific to ECT2.

To determine in which stages of the cell cycle ECT2 is induced, we synchronized T98G human glioblastoma cells and followed the ECT2 expression in the cell cycle. As shown in

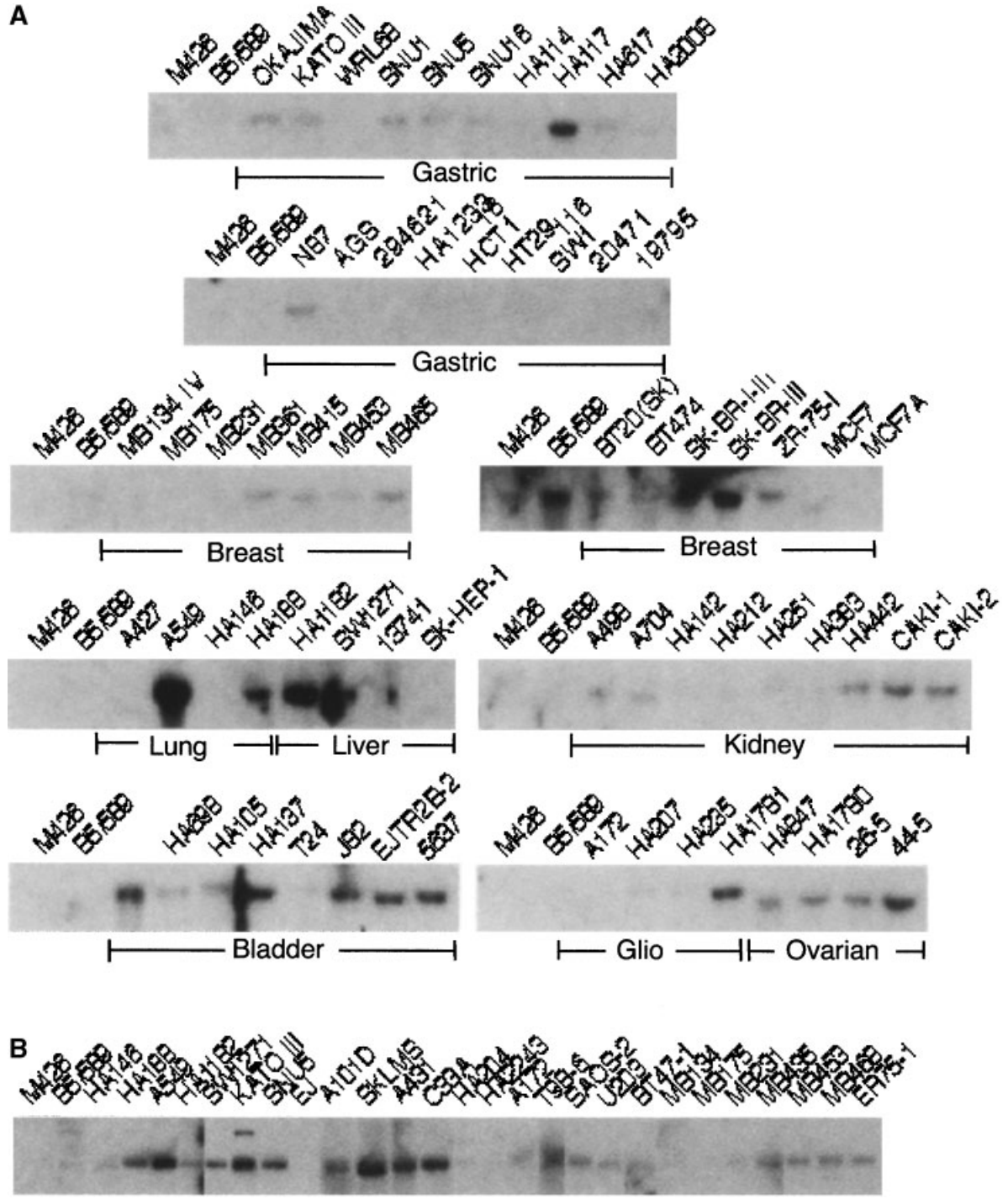

Fig. 2. Expression of *ECT2* in human tumor cell lines. **A**: *ECT2* mRNA expression in human tumor cell lines. RNA was extracted from the indicated cell lines, separated on a formaldehyde gel, and blotted onto a membrane. Each panel represents a single blot and the RNAs from two normal cell lines, M426 (lung fibroblasts) and B5/589 (epithelial cells), were included in each blot for references. The blots were hybridized with a 1.6-Kb SalI fragment containing the 3′-half of the human ECT2 cDNA 1M as probe. Equal loading of the RNA samples was confirmed by staining the rRNA species. **B**: ECT2 protein expression in human tumor cell lines. Lysates were prepared from the indicated cells, separated by SDS–PAGE, and blotted onto a nitrocellulose membrane. The blots were probed with anti-ECT2 antibody and visualized by a chemiluminescent system.

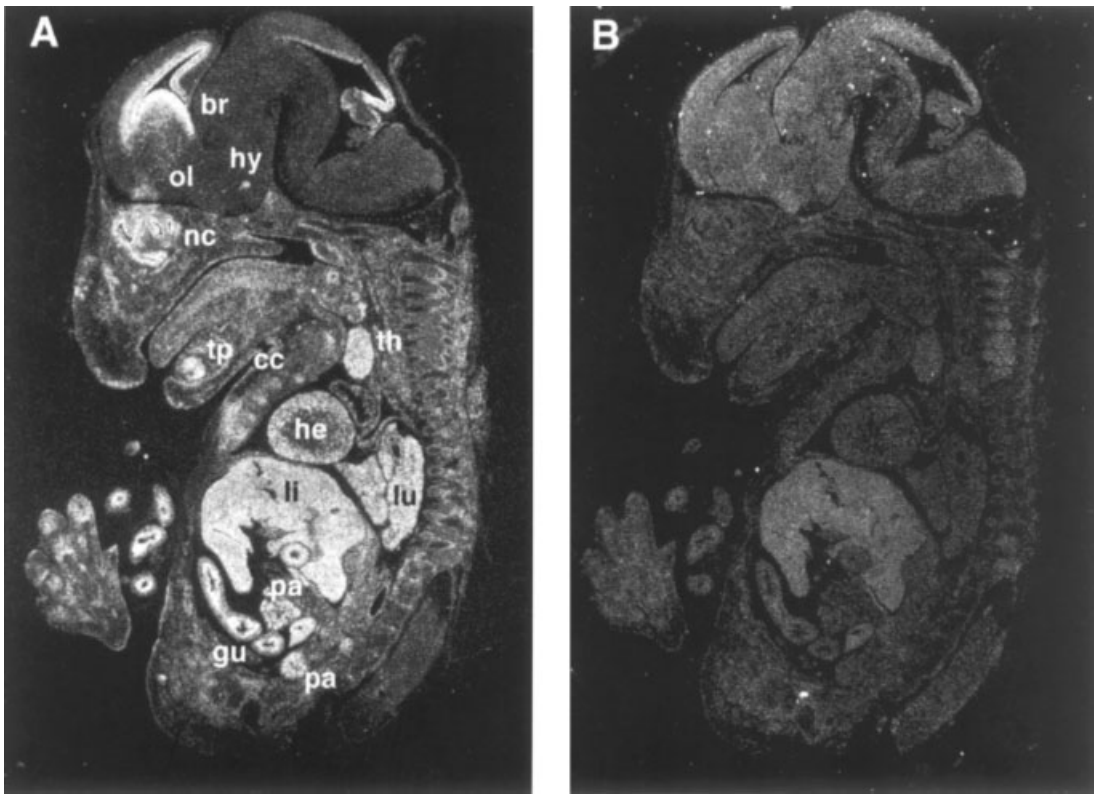

Fig. 3. Expression of *ect2* mRNA in mouse embryos. A sagittal section of a 14-day mouse fetus was used to hybridize with anti-sense strand (**A**) or sense strand (**B**) of the *ect2* probe. B: br, brain; ol, olfactory lobe; hy, hypothalamus; nc, nasal cavities; tp, tooth primordium; th, thymus; he, heart; li, liver; lu, lung; cc, costal cartilage; pa, pancreas; gu, gut.

Figure 4B, ECT2 expression is induced as early as 6 h after serum addition, and reached to a peak 27–30 h after induction. Flow cytometric analyses indicated that the majority of the cells were in S phase 24 h after induction, whereas the percentage of cells in G2/M phases were the highest 27–30 h after serum induction under these conditions. These results suggest that ECT2 expression is induced at S phase by serum and reached to the maximum at late S phase and G2/M phases. Examination of ECT2 mRNA revealed a similar expression pattern (Fig. 4C), suggesting that ECT2 expression is regulated at the transcriptional level.

ECT2 Expression Is Regulated by Various Growth Factors

To further investigate the regulation of *ECT2* expression during cell proliferation, we examined whether ECT2 is also induced by growth factors. We first monitored mouse *ect2* in serum-starved Balb/MK cells following the addition of keratinocyte growth factor (KGF), an epithelial cell-specific mitogen [Rubin et al., 1989]. In

Fig. 4. Induction of ECT2 by serum. **A**: Immunocytochemical detection of ECT2 before and after serum induction. M426 cells were stained for endogenous ECT2 by anti-ECT2 antibodies before and after serum-induction (**upper panels**). Nuclei of the cells were also stained with DAPI (**lower panels**). Similar experiments for NIH 3T3 mouse embryonic fibroblasts exhibited similar results. **B**: ECT2 protein expression in response to serum stimulation. T98G cells starved in 0.1% FBS for 72 h were stimulated to re-enter the cell cycle by the addition of fresh medium containing 10% FBS. Samples were harvested at the indicated time points, and analyzed by Western immunoblotting using the indicated antibodies. The blot was reprobed with anti-α-tubulin antibody to confirm equal loading of cellular components. A cell cycle profile is also shown, which contains percentages of cells in G0/G1, S, and G2/M phases at each time point obtained by flow cytometry. **C**: ECT2 mRNA expression in response to serum stimulation. Total RNA was extracted at the same time points as shown in (A) and analyzed by Northern blotting using ECT2-N4 cDNA as probe. 28S ribosomal RNA was also detected for a loading control.

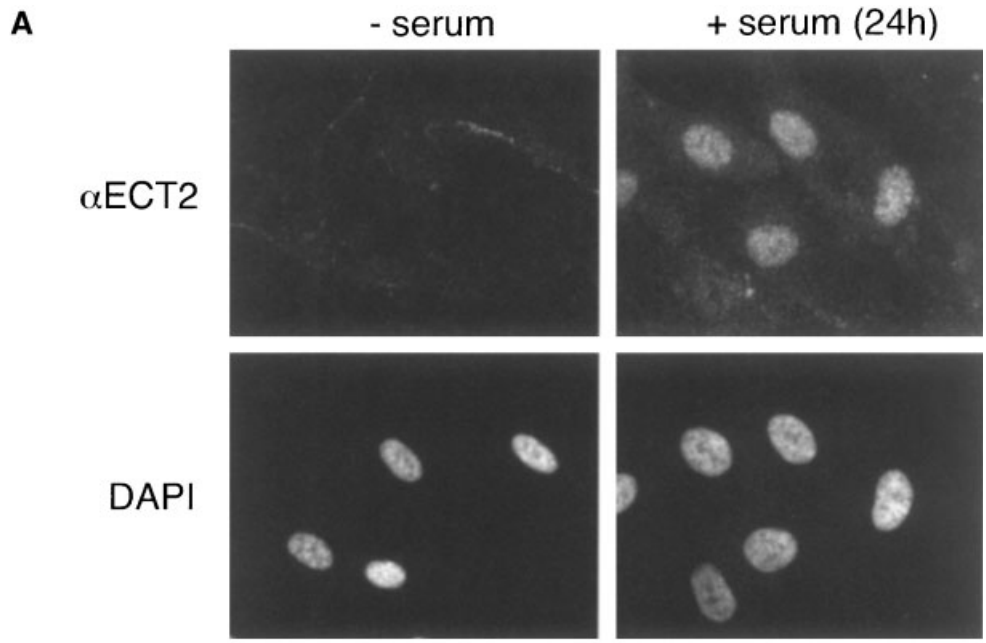

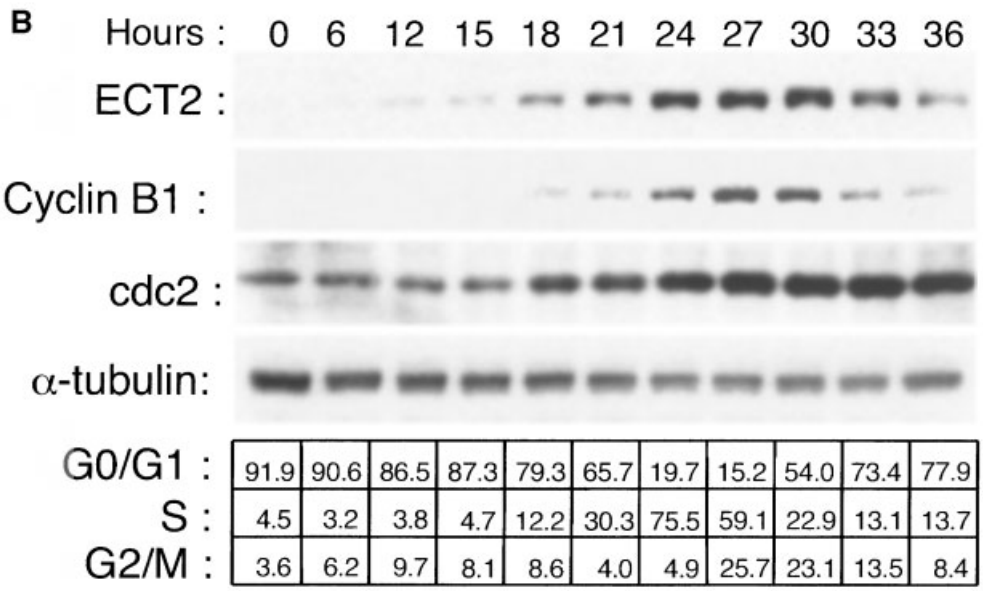

G0/G1 :	91.9	90.6	86.5	87.3	79.3	65.7	19.7	15.2	54.0	73.4	77.9
S :	4.5	3.2	3.8	4.7	12.2	30.3	75.5	59.1	22.9	13.1	13.7
G2/M :	3.6	6.2	9.7	8.1	8.6	4.0	4.9	25.7	23.1	13.5	8.4

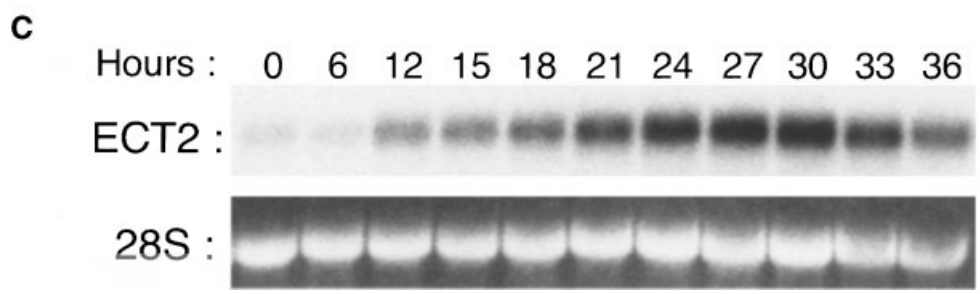

Fig. 4.

serum-starved Balb/MK cells, the expression of *ect2* was barely detectable (Fig. 5A, left panel). However, stimulation of Balb/MK by KGF resulted in a gradual increase that reached a peak after 48 h (9.7-fold increase when normalized with GAPDH signals). Ect2 transcript was induced by KGF at a concentration of 1 ng/ml and increased in a dose-dependent manner (Fig. 5A, right panel). A large induction of ~100 kDa Ect2 protein was observed in response to KGF in a time- and dose-dependent fashion (Fig. 5B). To determine in which phase of the cell cycle Ect2 was induced, we measured DNA synthesis following KGF treatment. The onset of Ect2 induction by KGF coincided with initiation of DNA synthesis determined by ^{3}H-thymidine incorporation (Fig. 5C). Similar to the induction kinetics by serum induction, *ect2* induction was reached the maximum level after the peak of DNA synthesis.

To further test this correlation, we examined the effect of transforming growth factor-β (TGF-β) on Ect2 expression. Consistent with its antiproliferative activity on Balb/MK cells, TGF-β did not promote Ect2 expression during 48 h of treatment (Fig. 5D). Moreover, concomitant exposure to KGF and TGF-β caused a delay in the onset of Ect2 induction relative to the pattern seen with KGF alone (compare Fig. 5D, lower panel with Fig. 5A, left panel). A similar delay was observed in the onset of DNA synthesis (data not shown).

Another mitogen for Balb/MK, epidermal growth factor (EGF), also exhibited a similar effect on *ect2* induction (Fig. 6A, lane 4). In contrast, hepatocyte growth factor (HGF)/scatter factor (SF) or insulin-like growth factor I (IGF-I) did not induce *ect2* expression significantly even at higher concentrations than KGF (lanes 5 and 6). However, when these growth factors were added together, they could potently induce *ect2* expression (lane 7). These results were consistent with the observation that HGF/SF and IGF-I are weak mitogens for Balb/MK cells when tested separately, but have a potent synergistic effect when used in combination (Fig. 6B). Thus, there was a correlation between the stimulation of DNA synthesis and induction of Ect2.

We also found that platelet-derived growth factor (PDGF), the major mitogen in serum, induced *ECT2* expression in a time-dependent manner (data not shown). Stimulation of fibroblasts with interleukin 1α, a cytokine with potent proinflammatory activity, weakly elevated *ECT2* mRNA levels, but transforming growth factor α (TGF-α), a mitogen with activities in fibroblasts and epithelial cells, caused no significant variation in the levels of *ECT2* mRNA (data not shown).

ECT2-N Expression Generates Cells With High DNA Contents

We have previously shown that ECT2-N can function as a dominant negative form of ECT2 and inhibits cytokinesis to generate multinucleate cells. To examine the inhibitory effect of ECT2-N on cytokinesis in detail, we utilized a flow cytometric analysis. U2OS cells were transiently transfected with the ECT2-N4 expression vector (see Fig. 8A) together with an expression vector for the membrane marker protein CD56, and then DNA contents of CD56-positive cells were analyzed by flow cytometry (Fig. 7A). Vector alone or an expression vector for $p21^{WAF1}$ was used as controls. The vector alone transfectants were detected as peaks of cells with 2N and 4N DNA content, which represent G1 and G2 cells, respectively, whereas the majority of $p21^{WAF1}$ transfectants were in the 2N peak, indicating that these cells arrested in G1. In contrast to the vector alone transfectants, ECT2-N4-expressing cells exhibited a higher population of 4N cells than that of 2N cells. Moreover, 48 h after transfection, ECT2-N4 transfectants also contained cells with DNA contents higher than 4N, suggesting that these cells contain multiple nuclei. Concomitant to a decrease of the peaks of 2N and 4N cells of ECT2-N4 transfectants 96 h after transfection, an increase of the 8N and 16N peaks was observed (Fig. 7A). These results suggest that the accumulation of cells with 4N DNA content was a transient event, and these 4N cells subsequently became 8N and 16N cells. When ECT2-N4 expressing cells were treated with nocodazole, a microtubule de-stabilizing agent which arrests the cells at M phase, the generation of cells with 8N DNA content by ECT2-N expression was efficiently inhibited (Fig. 7B), suggesting that 8N cells were produced from 4N cells through M phase progression without cytokinesis. Similar effects of the expression of ECT2-N4 were also observed in other cell lines including HCT116, A549, and MCF7 (Fig. 8A), suggesting that the formation of cells with higher DNA contents is not a cell line-dependent event. ECT2-N4 was efficiently

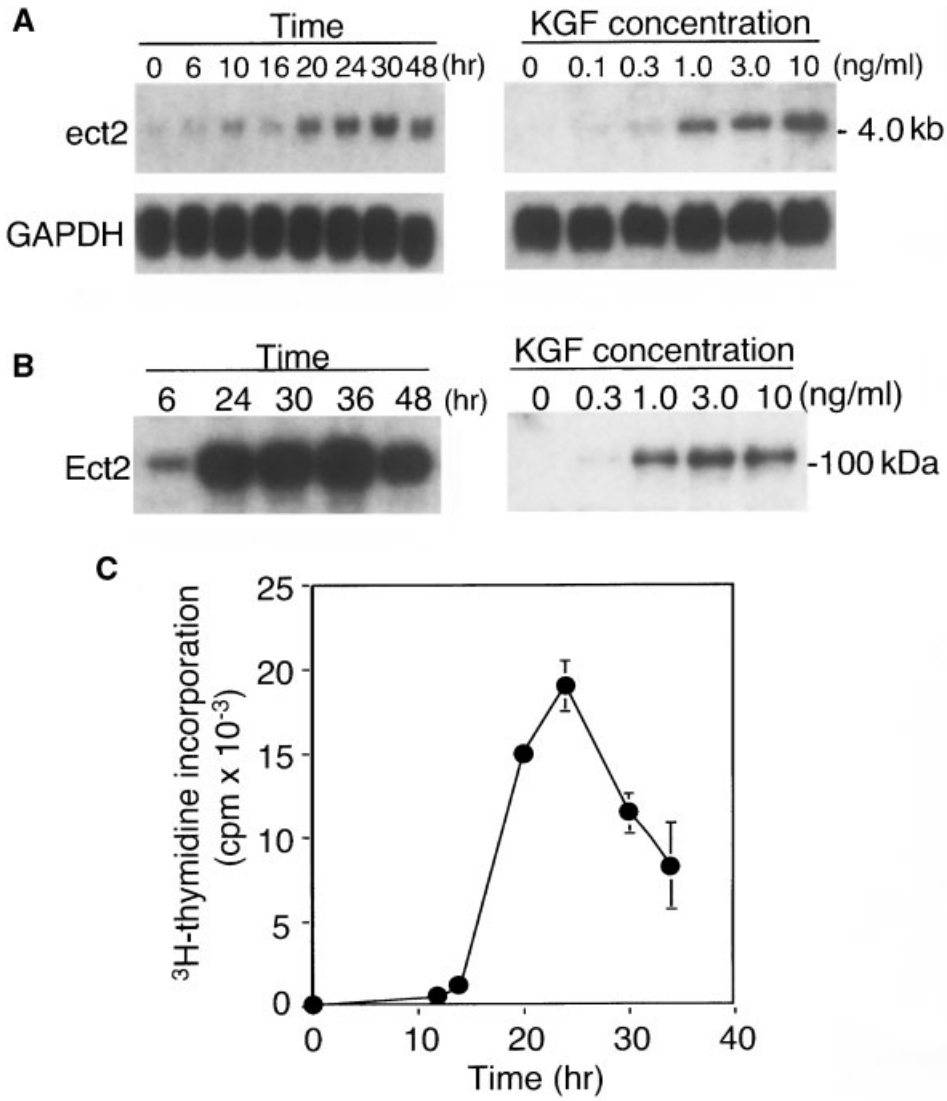

Fig. 5. Induction of *ect2* mRNA and protein in Balb/MK cells. **A** (**left panel**): Expression of *ect2* mRNA after addition of KGF to Balb/MK cells. Serum-starved Balb/MK cells were treated with KGF (20 ng/ml) and then harvested at the indicated time points. RNAs were analyzed by Northern blot hybridization with a mouse *ect2* cDNA as probe. GAPDH mRNA was monitored to assure similar loading of samples. Shown is a representative result of two independent experiments. **Right panel**: Dose-response effect of KGF on *ect2* mRNA expression. Quiescent Balb/MK cells were treated with various concentrations of KGF (0–10 ng/ml) for 30 h and *ect2* transcript was analyzed by Northern blot hybridization. **B** (**left panel**): Time course of Ect2 protein induction by KGF (10 ng/ml) in Balb/MK cells. **Right panel**: Dose-dependent induction of Ect2 protein by KGF in Balb/MK cells. Molecular size is indicated at the right. **C**: Kinetics of ^{3}H-thymidine incorporation in Balb/MK cells after treatment with KGF (3 ng/ml). Mean values ± SD of triplicate measurements are shown. Shown is a representative result of two independent experiments. **D**: Effect of TGF-β on *ect2* mRNA expression. Serum-starved Balb/MK cells were treated with TGF-β (1 ng/ml) alone or KGF (10 ng/ml) plus TGF-β (1 ng/ml) for the indicated time periods. RNAs were visualized by Northern blot analysis with *ect2* or GADPH cDNA probes. Shown is a representative result of two independent experiments.

expressed in U2OS, HCT116, and A549 (Fig. 8B). In MCF7, ECT2-N4 expression was lower than in other cell lines, and only a slight increase of the 4N peak was observed. Expression of ECT2-F in U2OS cells also exhibited the higher 4N peak than the 2N peak 48 h after transfection (Fig. 7A), but cells with DNA content of higher than 4N were not observed 96 h after transfection.

Cytoplasmic Localization of ECT2-N Stimulates Multinucleate Cell Formation

Using the flow cytometric analysis, we examined the effects of various ECT2-N derivatives

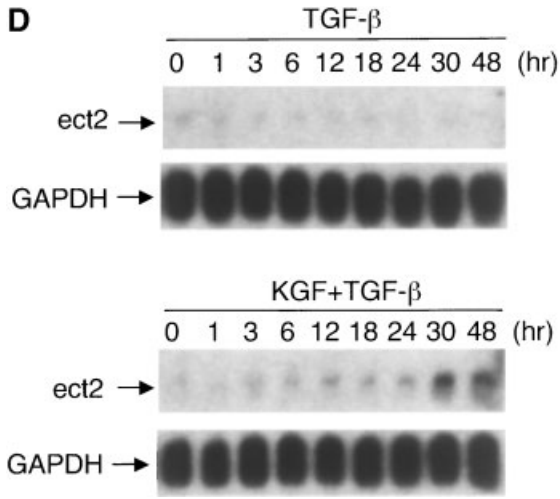

Fig. 5. (*Continued*)

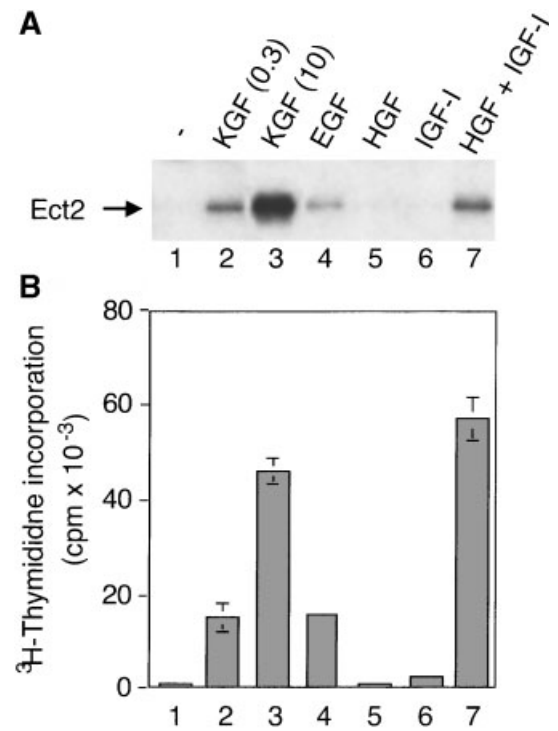

Fig. 6. Induction of Ect2 protein by growth factors. **A**: Immunoblot analysis of Ect2 in Balb/MK cells in serum free medium in the absence of growth factors (**lane 1**), or in the presence of 0.3 ng/ml KGF (**lane 2**), 10 ng/ml KGF (**lane 3**), 10 ng/ml EGF (**lane 4**), 20 ng/ml HGF/SF (**lane 5**), 200 ng/ml IGF-I (**lane 6**), or 20 ng/ml HGF/SF plus 200 ng/ml IGF-I (**lane 7**). **B**: Stimulation of DNA synthesis in growth factor-treated Balb/MK cells. Cultures were treated with various mitogens as in (A). DNA synthesis was measured by ^{3}H-thymidine incorporation. Shown are the mean values ± SD of triplicate measurements from a representative experiment. Two independent experiments were performed.

on cytokinesis. ECT2 contains two putative nuclear localization signals (NLSs) in a small central region, designated the S domain (Fig. 9A). We expressed ECT2-N derivatives as green fluorescent protein (GFP)-fusion proteins, and examined their subcellular localization (Fig. 9B). ECT2-F and ECT2-N1, which contain the intact S domain and thus both the NLSs, were predominantly localized in the nucleus. However, ECT2-N3, which contains only one of the NLSs, exhibited cytoplasmic localization, although the majority of the protein was still localized in the nucleus. In contrast to these proteins, ECT2-N4, which lacks both the NLSs, was localized in the cytoplasm as well as the nucleus. GFP alone was also localized to both the cellular compartments.

To test whether the subcellular localization affects the dominant negative effect of the ECT2-N proteins, DNA content of the transfectants was analyzed by flow cytometry as described above. To avoid the effects of cellular damage caused by transfection reagents, we estimate DNA content 72–90 h after transfection. While ECT2-N1 and ECT2-N2 as well as ECT2-F did not exhibit significant accumulation of cells with higher DNA content, ECT2-N3 and ECT2-N4 caused an increase of 4N cells and appearance of 8N and 16N cells (Fig. 9A). The effect of ECT2-N4 on the generation of multinucleate cells was significantly higher than ECT2-N3, supporting the correlation between cytoplasmic localization and cytokinesis inhibition. The expression level of these GFP-ECT2 fusion proteins was comparable (Fig. 9C). These results suggest that cytoplasmic localization of ECT2-N strongly enhances the ability of ECT2-N to inhibit cytokinesis.

Cell Cycle/Repair Domains in ECT2-N Are all Required for Efficient Cytokinesis Inhibition

We further tested which cell cycle/repair domains in ECT2-N are responsible for cytokinesis inhibition. For this purpose, a deletion or mutation was introduced in each of the domains in ECT2-N4, which exhibited a strong inhibitory effect on cytokinesis. Interestingly, changes of the conserved amino acid residues (THL to AAA) in either of the BRCT repeats of ECT2-N4 efficiently abolished the appearance of multinucleated cells (Fig. 9A), suggesting that each of these repeats is essential for the inhibition of cytokinesis. Additionally, ECT2-

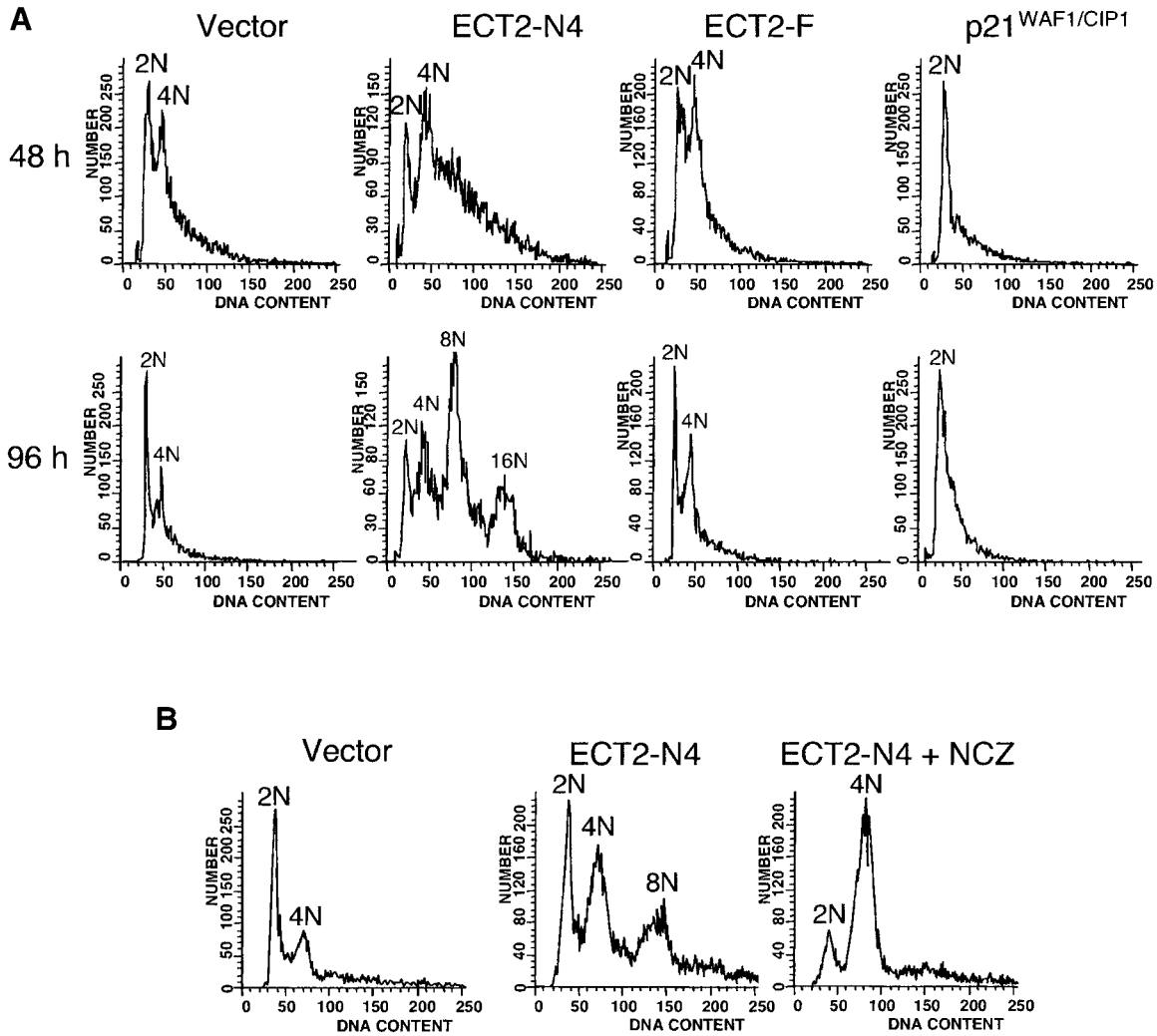

Fig. 7. Analysis of DNA content of U2OS cells expressing ECT2. **A**: U2OS cells were transiently transfected with the empty vector or the ECT2-N4 or $p21^{WAF1}$ expression vector, together with the CD56 expression vector. Transfectants were FACS-sorted for CD56 marker expression and their DNA contents analyzed following propidium iodide staining 48 h (**upper panels**) or 96 h (**lower panels**) after transfection. **B**: U2OS cells were transfected with the ECT2-N4 and CD56 expression vectors and cultured as above except that nocodazole was added at a final concentration of 0.4 μg/ml, 18 h after transfection (+NCZ). Transfectants were FACS-sorted for CD56 marker expression and their DNA contents analyzed following propidium iodide staining 72 h after transfection.

N5, an ECT2-N4 derivative lacking the C-terminal half of BRCT repeat 2, did not significantly inhibit cytokinesis. Moreover, a small internal deletion in the CLB6 domain or an N-terminal deletion extending to the XRCC1 domain also abolished the ability of ECT2-N to inhibit cytokinesis. In contrast, a small N-terminal deletion (ECT2-N4ΔN), which does not extend to the XRCC1 domain, did not affect the activity. The expression level of these exogenous proteins was comparable as detected by immunoblotting using anti-ECT2 antibody (data not shown). These results strongly suggest that all of the XRCC1, CLB6, BRCT-1, and BRCT-2 domains play a crucial role in regulating cytokinesis.

DISCUSSION

Human ECT2 contains cell cycle regulator/checkpoint control protein-related domains in the N-terminal half. *Drosophila* Pbl and *C. elegans* T19E10.1b proteins exhibited structural similarities to ECT2 in the entire stretch of their open-reading frames, suggesting that these are fly and worm orthologs, respectively. These *ECT2* orthologs, as well as human Rad4-like (accession no. Z46795) and *C. elegans*

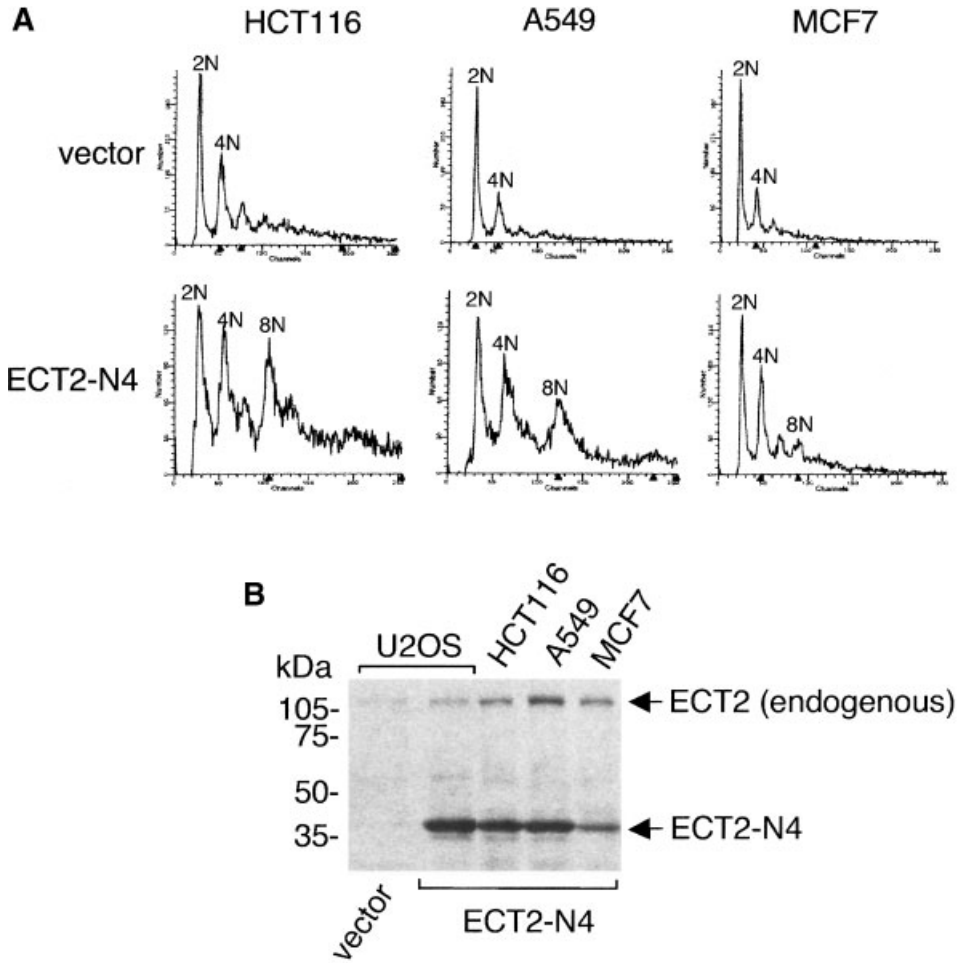

Fig. 8. Analysis of DNA content of HCT116, A549, and MCF7 expressing ECT2-N. **A**: HCT116 (human colon carcinoma), A549 (human lung carcinoma), and MCF7 (human mammary carcinoma) cells were transfected with ECT2-N4 or vector alone together with CD56, and analyzed as in the legend to Figure 1A, 96 h after transfection. **B**: Expression levels of endogenous ECT2 and exogenously expressed ECT2-N4 as detected by immunoblotting by anti-ECT2 antibody.

F37D6.1 (accession no. Z75540) genes, contain the BRCT repeats, which are also found within many DNA damage repair and cell cycle checkpoint control proteins [Bork et al., 1997]. BRCT domains are 85–95 amino acid domains that comprise several distinct clusters of conserved hydrophobic amino acids that together form the core of the BRCT fold [Huyton et al., 2000]. There is no invariant amino acid residue throughout the whole BRCT superfamily and this lack of sequence identity makes recognition of distant family members difficult. However, the comparison of the domains among those which are most homologous to ECT2 suggests several conserved regions (Fig. 1C). The N-terminal tandem BRCT repeats of Cut5 interact

Fig. 9. Determination of the domains responsible for multinucleate cell formation by ECT2-N. **A**: Structure of ECT2 derivatives and their ability to generate multinucleate cells. Regions carried by ECT2 expression vectors are shown below the schematic structure of ECT2. Location and amino acid sequence of tandem NLSs are also shown. Numbers denote amino acid numbers. X indicates location of mutations (THL to AAA). The positions of these mutations are also shown by ''***'' in Figure 1B. Multinucleate cell generation was estimated by flow cytometry as in the legend to Figure 7. −, <5%; +, 20 ~ 50%; ++, >50% of 8N and 16N cells in the CD56 positive cell population. **B**: Subcellular localization of GFP-ECT2 fusion proteins. The cDNAs were cloned in pEGFPC1 vectors and used to transfect U2OS cells. Forty-eight hours after transfection, Hoechst 33342 dye was added to culture medium at a final concentration of 10 μM and cells were directly observed under the fluorescence microscope and photographed. The GFP fusion proteins and nucleus were visualized by green fluorescence and Hoechst 33342 (blue), respectively (magnification, 400×). Merged images are shown at the bottom. **C**: Expression levels of GFP-ECT2 fusion proteins. The fusion proteins were detected by anti-GFP antibody.

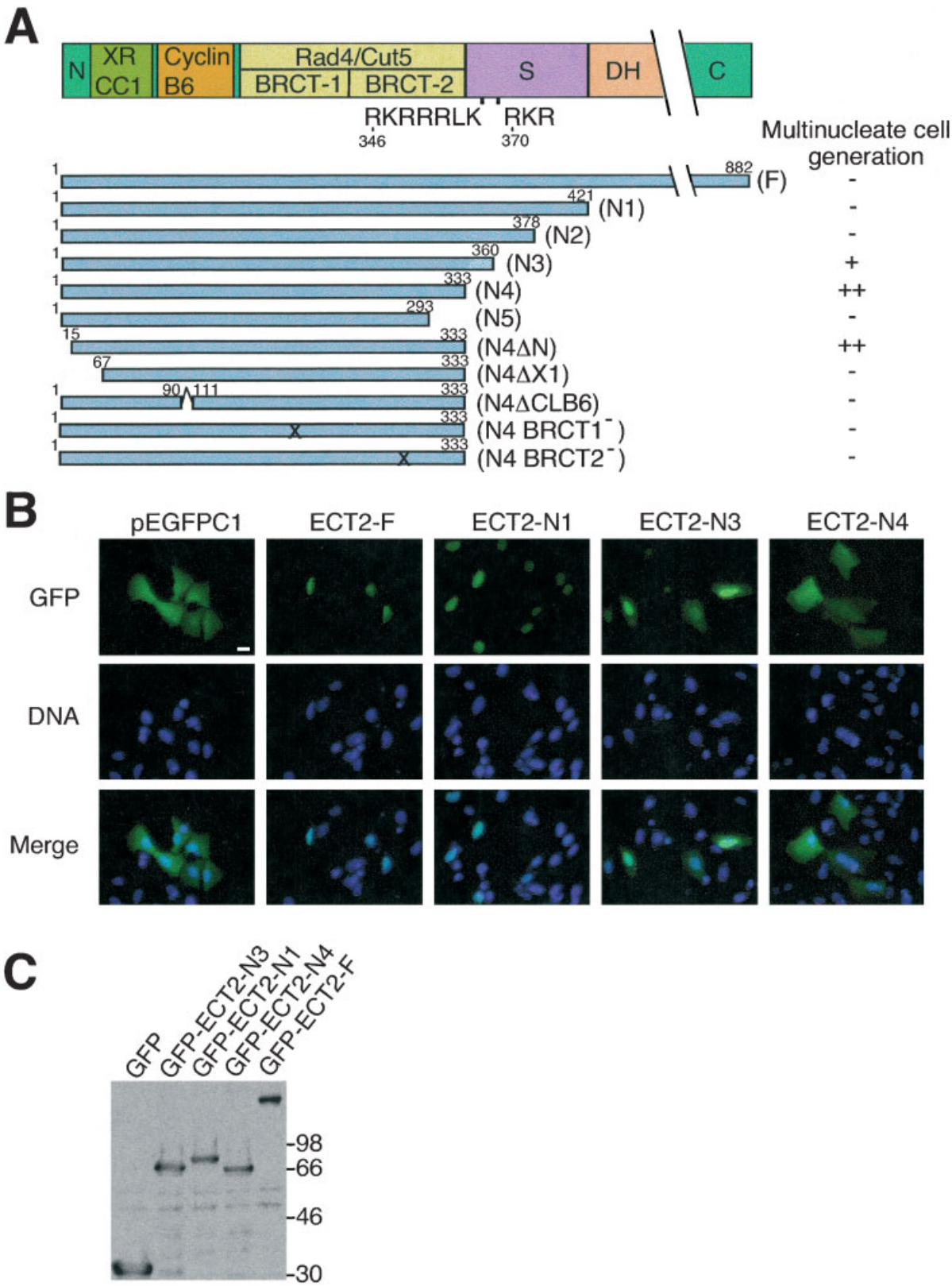
A
N
XR
CC1
Cyclin
B6
Rad4/Cut5
BRCT-1
BRCT-2
S
DH
C
RKRRRLK
346
RKR
370
Multinucleate cell generation
1
882
(F)
-
421
(N1)
-
378
(N2)
-
360
(N3)
+
333
(N4)
++
293
(N5)
-
15
(N4ΔN)
++
67
(N4ΔX1)
-
90
111
(N4ΔCLB6)
-
X
(N4 BRCT1⁻)
-
X
(N4 BRCT2⁻)
-
B
pEGFPC1
ECT2-F
ECT2-N1
ECT2-N3
ECT2-N4
GFP
DNA
Merge
C
GFP
GFP-ECT2-N3
GFP-ECT2-N1
GFP-ECT2-N4
GFP-ECT2-F
98
66
46
30

Fig. 9.

with another checkpoint control protein Crb2, which is closely related to the budding yeast checkpoint control protein Rad9 [Saka et al., 1997]. Since ECT2 BRCT domains are most homologous to the N-terminal two BRCT repeats of Cut5 among the known BRCT domains, ECT2 BRCT domains may also associate with certain molecules such as checkpoint control proteins to transmit the signals to downstream molecules.

The BRCT repeats in ECT2 were also closely related to those of the human repair protein XRCC1 [Thompson et al., 1990] and human topoisomerase II-binding protein TopBP1 [Yamane et al., 1997]. ECT2 also contains the XRCC1-related domain besides the BRCT repeats (Fig. 1). Recently, it has been shown that the *Xenopus* ortholog of human TopBP1 is involved in initiation of DNA replication through chromatin binding [Hashimoto and Takisawa, 2003]. A domain homologous to the yeast S phase cyclin CLB6 was identified in ECT2 between the XRCC1 domain and the BRCT repeats. The new type pair of yeast B-cyclins CLB5 and CLB6 are involved in DNA replication [Schwob and Nasmyth, 1993]. An interesting finding is that these cyclins are required for premeiotic DNA replication and activation of the meiotic S/M checkpoint [Stuart and Wittenberg, 1998]. As ECT2 is localized in the nucleus of interpahse cells [Tatsumoto et al., 1999], ECT2 may function in DNA replication, repair, and/or checkpoint control through the XRCC1, CLB6, and BRCT domains.

ECT2 expression was markedly high in mouse embryonic tissues containing rapidly proliferating cells. Moreover, ECT2 is also expressed at high levels in various tumor cell lines, which are also growing rapidly. Most of the ovarian and bladder carcinomas examined, exhibited elevated ECT2 expression. The expression level of ECT2 was highest in a lung carcinoma cell line A549 and colon carcinoma SW480. These results may indicate that elevated ECT2 expression stimulates cell proliferation. In contrast to the overexpression of ECT2 in various tumor cell lines, there was no evidence for structural alterations of the gene, although more studies will be needed to solve the question. Stimulation of resting cells to reenter the cell cycle by serum and growth factors is followed by a rapid, and sometimes transient, activation of a group of primary response genes, whose expression is believed to initiate and to be critical for the establishment of the cellular responses to these stimuli. Our results demonstrated that serum and several growth factors promoted a significant elevation of ECT2 expression. Unlike immediate early genes that are induced by serum at G1 phase, ECT2 induction occurred in S phase and gradually increases towards its maximum in G2/M. Increase of both ECT2 mRNA and protein in S, G2, and M phases of the cell cycle suggests a possible function of *ECT2* in these phases of the cell cycle. As the present results support that ECT2 is a critical regulator of cytokinesis, increased expression of ECT2 in M phase is consistent with its biological function. However, induction of ECT2 is in coincidence with the onset of S phase, suggesting that ECT2 may have an additional function in S phase. As discussed above, the BRCT motif provided impetus for the present study because of the association of this domain with proteins that participate in checkpoint control of the cell cycle.

We examined the effect of ECT2-N on cell division in U2OS cells using flow cytometry. The majority of cells expressing ECT2-N were detected as cells with 4N or higher DNA contents, which is consistent with the previous result that ECT2-N can function as a dominant negative mutant and induces multinucleate cell formation [Tatsumoto et al., 1999]. Using this assay, we found a correlation between cytoplasmic localization of ECT2-N and inhibition of cytokinesis. ECT2 disperses to the entire cells after nuclear membrane breakdown and then accumulates in the midbody [Tatsumoto et al., 1999]. To display the dominant negative effect towards cytokinesis, ECT2-N must compete with endogenous ECT2 for binding to the sites where it regulates cytokinesis. When ECT2-N is present in the cytoplasm before nuclear membrane breakdown, it may pre-emptively occupy the ECT2 binding sites, which will later become a component of the regulatory site for cytokinesis. Therefore, it is likely that ECT2-N derivatives lacking NLSs can localize in the cytoplasm before the endogenous ECT2 reaches to this compartment, and therefore, can strongly display its dominant-negative effect to inhibit cytokinesis.

Mutational analysis revealed that each of XRCC1, CLB6, BRCT-1, and BRCT-2 domains is required for the inhibitory effect of ECT2-N on cytokinesis. Thus, these domains might play a critical role to regulate cytokinesis by ECT2.

The BRCT motif can function as a protein–protein interaction site as discussed above. Besides the BRCT domains, the XRCC1 homology domain may also have such a function. The CLB6 domain is homologous to a region of budding yeast cyclin B6 between the cyclin box and destruction box. This region may also function as a binding site to other proteins. Collectively, the cell cycle/repair domains of ECT2 may function as the binding sites of upstream signaling molecules and/or scaffold proteins, which can determine the localization of ECT2 to the site where it regulates cytokinesis. As N-terminal truncation of ECT2 activates its transforming activity [Miki et al., 1993], ECT2-N appears to interact with the catalytic domain to negatively regulate the exchange activity. Therefore, association of ECT2 at its N-terminal domain with upstream molecules may activate the exchange activity of ECT2 by dissolving the negative regulation. Some of the upstream molecules may localize at the site for cytokinesis. Thus, such a regulatory mechanism may allow ECT2 to activate Rho GTPases at a spatiotemporal manner, which is required for the precise control of cytokinesis. Further studies of ECT2 and identification of its binding proteins will clarify the molecular mechanisms of cytokinesis as well as yet undiscovered functions of ECT2.

ACKNOWLEDGMENTS

We thank Dr. J. Pierce, Dr. L. Samelson, and Dr. D. Lowy for support; Dr. Cecil Fox for assistance with in situ hybridization; Dr. Jerry Ward for discussion of *ect2* expression in embryos; and Ricardo Dreyfuss for photography. T.T was supported by Japan Society of Promotion of Sciences fellowships for Biomedical and Behavioral Researchers in NIH.

REFERENCES

Bork P, Hofmann K, Bucher P, Neuwald AF, Altschul SF, Koonin EV. 1997. A superfamily of conserved domains in DNA damage-responsive cell cycle checkpoint proteins. FASEB J 11:68–76.

Cioce V, Csaky KG, Chan AM, Bottaro DP, Taylor WG, Jensen R, Aaronson SA, Rubin JS. 1996. Hepatocyte growth factor (HGF)/NK1 is a naturally occurring HGF/scatter factor variant with partial agonist/antagonist activity. J Biol Chem 271:13110–13115.

Fox CH, Cottler-Fox M. 1993. In situ hybridization in HIV research. Microsc Res Tech 25:78–84.

Hall A. 1998. Rho GTPases and the actin cytoskeleton. Science 279:509–514.

Hashimoto Y, Takisawa H. 2003. *Xenopus* Cut5 is essential for a CDK-dependent process in the initiation of DNA replication. EMBO J 22:2526–2535.

Huyton T, Bates PA, Zhang X, Sternberg MJ, Freemont PS. 2000. The BRCA1 C-terminal domain: Structure and function. Mutat Res 460:319–332.

Kimura K, Tsuji T, Takada Y, Miki T, Narumiya S. 2000. Accumulation of GTP-bound RhoA during cytokinesis and a critical role of ECT2 in this accumulation. J Biol Chem 275:17233–17236.

Lorenzi MV, Castagnino P, Chen Q, Hori Y, Miki T. 1999. Distinct expression patterns and transforming properties of multiple isoforms of Ost, an exchange factor for RhoA and Cdc42. Oncogene 18:4742–4755.

Miki T, Smith C, Long J, Eva A, Fleming T. 1993. Oncogene *ect*2 is related to regulators of small GTP-binding proteins. Nature 362:462–465.

Prokopenko SN, Brumby A, O'Keefe L, Prior L, He Y, Saint R, Bellen HJ. 1999. A putative exchange factor for Rho1 GTPase is required for initiation of cytokinesis in *Drosophila*. Genes Dev 13:2301–2314.

Ron D, Bottaro DP, Finch PW, Morris D, Rubin JS, Aaronson SA. 1993. Expression of biologically active recombinant keratinocyte growth factor. Structure/function analysis of amino-terminal truncation mutants. J Biol Chem 268:2984–2988.

Rubin JS, Osada H, Finch PW, Taylor WG, Rudikoff S, Aaronson SA. 1989. Purification and characterization of a newly identified growth factor specific for epithelial cells. Proc Natl Acad Sci USA 86:802–806.

Saito S, Inoue T, Kawase I, Hara H, Tanio Y, Tachibana I, Hayashi S, Watanabe M, Matsunashi M, Osaki T, Masuno T, Kishimoto S. 1991. Two monoclonal antibodies against small-cell lung cancer show existence of synergism in binding. Cancer Immunol Immunother 33:165–170.

Saito S, Tanio Y, Tachibana I, Hayashi S, Kishimoto T, Kawase I. 1994. Complementary DNA sequence encoding the major neural cell adhesion molecule isoform in a human small cell lung cancer cell line. Lung Cancer 10: 307–318.

Saka Y, Yanagida M. 1993. Fission yeast cut5+, required for S phase onset and M phase restraint, is identical to the radiation-damage repair gene *rad4*$^{+}$. Cell 74:383–393.

Saka Y, Fantes P, Sutani T, McInerny C, Creanor J, Yanagida M. 1994. Fission yeast *cut5* links nuclear chromatin and M phase regulator in the replication checkpoint control. EMBO J 13:5319–5329.

Saka Y, Esashi F, Matsusaka T, Mochida S, Yanagida M. 1997. Damage and replication checkpoint control in fission yeast is ensured by interactions of Crb2, a protein with BRCT motif, with Cut5 and Chk1. Genes Dev 11: 3387–3400.

Sakata H, Rubin JS, Taylor WG, Miki T. 2000. A Rho-specific exchange factor Ect2 is induced from S to M phases in regenerating mouse liver. Hepatology 32:193–199.

Schwob E, Nasmyth K. 1993. CLB5 and CLB6, a new pair of B cyclins involved in DNA replication in *Saccharomyces cerevisiae*. Genes Dev 7:1160–1175.

Stuart D, Wittenberg C. 1998. CLB5 and CLB6 are required for premeiotic DNA replication and activation of the meiotic S/M checkpoint. Genes Dev 12:2698–2710.

Takai S, Long JE, Yamada K, Miki T. 1995. Chromosomal localization of the human *ECT2* proto-oncogene to 3q26.1−>q26.2 by somatic cell analysis and fluorescence in situ hybridization. Genomics 27:220–222.

Tatsumoto T, Xie X, Blumenthal R, Okamoto I, Miki T. 1999. Human ECT2 is an exchange factor for Rho GTPases, phosphorylated in G2/M phases, and involved in cytokinesis. J Cell Biol 147:921–927.

Thompson LH, Brookman KW, Jones NJ, Allen SA, Carrano AV. 1990. Molecular cloning of the human XRCC1 gene, which corrects defective DNA strand break repair and sister chromatid exchange. Mol Cell Biol 10: 6160–6171.

Van Aelst L, D'Souza-Schorey C. 1997. Rho GTPases and signaling networks. Genes Dev 11:2295–2322.

Yamane K, Kawabata M, Tsuruo T. 1997. A DNA-topoisomerase-II-binding protein with eight repeating regions similar to DNA-repair enzymes and to a cell-cycle regulator. Eur J Biochem 250:794–799.